Exact solutions for the flow of Casson fluid over a stretching surface with transpiration and heat transfer effects*

Swati Mukhopadhyay[a)†], Krishnendu Bhattacharyya[a)], and Tasawar Hayat[b)c)]

[a)] *Department of Mathematics, The University of Burdwan, Burdwan-713104, W. B., India*
[b)] *Department of Mathematics, Quaid-i-Azam University 45320, Islamabad, Pakistan*
[c)] *Department of Mathematics, Faculty of Science, King Abdulziz University, Jeddah 21589, Saudi Arabia*

(Received 26 March 2013; revised manuscript received 20 May 2013)

The effects of transpiration on forced convection boundary layer non-Newtonian fluid flow and heat transfer toward a linearly stretching surface are reported. The flow is caused solely by the stretching of the sheet in its own plane with a velocity varying linearly with the distance from a fixed point. The constitutive relationship for the Casson fluid is used. The governing partial differential equations corresponding to the momentum and energy equations are converted into non-linear ordinary differential equations by using similarity transformations. Exact solutions of the resulting ordinary differential equations are obtained. The effect of increasing Casson parameter, i.e., with decreasing yield stress (the fluid behaves as a Newtonian fluid as the Casson parameter becomes large), is to suppress the velocity field. However, the temperature is enhanced as the Casson parameter increases. It is observed that the effect of transpiration is to decrease the fluid velocity as well as the temperature. The skin-friction coefficient is found to increase as the transpiration parameter increases.

Keywords: stretching surface, transpiration, Casson fluid, heat transfer

PACS: 47.15.Cb, 44.20.+b, 47.50.–d **DOI:** 10.1088/1674-1056/22/11/114701

1. Introduction

The boundary layer flow over a stretching surface is often encountered in many engineering disciplines. During a manufacturing process, a stretched sheet interacts with the ambient fluid both thermally and mechanically.[1] Therefore, at the stretching surface, the flow behavior, which determines the rate of cooling, is an important aspect nowadays.[2] Further, flow and heat transfer phenomena over a stretching surface has promising applications in a number of technological processes including the production of polymer films or thin sheets.[3] Crane[4] investigated the steady flow of an incompressible viscous fluid over an elastic sheet, the flow being caused solely by the stretching of the sheet in its own plane with a velocity varying linearly with the distance from a fixed point. Heat transfer in a flow over a stretching surface maintained at constant and variable temperatures was investigated by Carragher and Crane[5] and Gupta and Gupta.[6] The work of Crane was subsequently extended by many authors to Newtonian/non-Newtonian boundary layer flow with various velocities and thermal boundary conditions.[7–10]

The Newtonian fluid model predicts a linear relationship between the shear stress and the velocity gradient. Due to the inadequacy of the Newtonian concept of fluids, many non-Newtonian fluid models have been proposed to explain complex behaviors. The constitutive relations of such models inherit complexities and lead to highly nonlinear equations of motion containing many terms. A simple alternative to these extremely complex equations is the boundary layer theory, which effectively reduces the complexity of Navier–Stokes equations and also drastically reduces the computational time. Analysis of the heat transfer due to a continuously stretching surface through an ambient fluid is one of the main thrusts of current research.[11] Further, heat transfer analysis plays a vital role during the handling and processing of non-Newtonian fluids. An assessment of technological applications requires the knowledge of the rheological characteristics of non-Newtonian fluids.[12] The flows of non-Newtonian fluids are very important due to their industrial and technological applications. For example, if one uses a non-Newtonian fluid as the coolant, the required pumping power might be greatly reduced. Therefore, a fundamental analysis of the flow field of non-Newtonian fluids in a boundary layer adjacent to a stretching sheet or an extended surface is very important, and is an essential part in the study of the fluid dynamics and heat transfer.[13] The differences between the features of non-Newtonian fluids and viscous fluids cannot be predicted by a single constitutive equation. Constitutive equations of viscoelastic fluids are generally classified into three types: differential, integral, and rate types. In the differential type, the deviatoric stress tensor is given explicitly in terms of the kinematic variables. In the integral type, the deviatoric stress tensor is written as an integral (or functional) of the kinematic variables. In the rate type, the deviatoric stress tensor, its rate of change, and its products with the kinematic vari-

*Project supported by UGC (New Delhi, India) through the Special Assistance Programme DSA Phase 1.
†Corresponding author. E-mail: swati_bumath@yahoo.co.in
© 2013 Chinese Physical Society and IOP Publishing Ltd

ables are all expressed as functions of the kinematic variables. Thus, several models of non-Newtonian fluids have been suggested in the literature, employing the differential, integral, or rate type equations.

In the literature, the vast majority of non-Newtonian fluid models are concerned with the simple models like the power law and grade two or three.[14–20] The simplest model for the rheological effects of rate type fluids is the Maxwell model where the dimensionless relaxation time is small and the stress relaxation can be predicted. Some recent investigations of Maxwell fluids are given in Refs. [21]–[23]. There is another non-Newtonian fluid model, known as the Casson fluid model. The Casson fluid can be defined as a shear thinning liquid which is assumed to have an infinite viscosity at zero rate of shear, a yield stress below which no flow occurs, and a zero viscosity at infinite rate of shear. Examples of the Casson fluid include jelly, tomato sauce, honey, soup, concentrated fruit juices, etc. In the literature, the Casson model is sometimes claimed to fit rheological data better than the general viscoplastic models for many materials. It has become the preferred rheological model for blood and chocolate. The Casson fluid exhibits a yield stress. If a shear stress less than the yield stress is applied to the fluid, it behaves like a solid, whereas if a shear stress greater than the yield stress is applied, it starts to move. Representative studies dealing with this model can be found in Refs. [24]–[27].

Fluid flow separation is an undesirable phenomenon, as the separation of the boundary layer is associated with large energy losses. In most applications, it adversely affects the aerodynamic loads in the form of lift loss and drag increase.[28–30] Therefore, in most systems involving fluid flows, in particular, underwater vehicles and turbo machinery, controlling the flow separation is very important. To control the flow separation, both passive and active devices have been used.[31,32] The process of suction/injection (blowing) is also important in many engineering applications, such as in the design of thrust bearings and radial diffusers and in thermal oil recovery. In chemical processes, suction is used to remove reactants whereas blowing is used to add reactants, cool the surfaces, prevent corrosion or scaling, and reduce drag.[33] Injection or withdrawal of fluid through a porous bounding wall that is either heated or cooled can lead to enhanced heating or cooling of the system and can help to delay a transition from the laminar flow.[34]

Motivated by the possible industrial applications and previous studies regarding the flow and heat transfer of non-Newtonian fluids over a stretching sheet, an analytical solution for the flow and heat transfer of a laminar boundary layer flow of Casson fluid subjected to suction/blowing is presented. By using similarity transformations, a third-order ordinary differential equation corresponding to the momentum equation and a second-order differential equation corresponding to the energy equation are derived. Exact solutions of the transformed momentum and energy equations are obtained. Numerical calculations are carried out for different values of dimensionless parameters of the problem to illustrate the results graphically. An analysis of the results shows that the flow field is influenced appreciably by the heat transfer parameter in the presence of suction or injection at the wall. It is expected that the results will both provide useful information for applications and complement the previous studies.

2. Governing equations

Consider the flow of an incompressible viscous fluid past a sheet coinciding with the plane $y = 0$. The fluid flow is confined to $y > 0$. Two equal and opposite forces are applied along the x axis so that the wall is stretched with the origin fixed (Fig. 1). The rheological equation of state for an isotropic and incompressible flow of a Casson fluid is

$$\tau_{ij} = \begin{cases} 2(\mu_{\mathrm{B}} + p_y/\sqrt{2\pi})e_{ij}, & \pi > \pi_{\mathrm{c}}, \\ 2(\mu_{\mathrm{B}} + p_y/\sqrt{2\pi_{\mathrm{c}}})e_{ij}, & \pi < \pi_{\mathrm{c}}, \end{cases} \tag{1}$$

where e_{ij} is the (i, j)-th component of the deformation rate, π is the product of the component of deformation rate with itself, $\pi = e_{ij}e_{ij}$, π_{c} is a critical value of this product based on the non-Newtonian model, μ_{B} is the plastic dynamic viscosity of the non-Newtonian fluid, and p_y is the yield stress of the fluid.

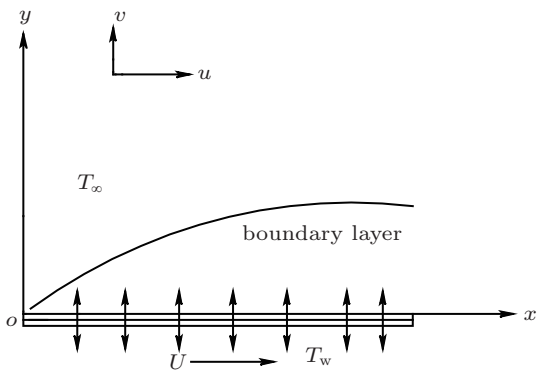


Fig. 1. Sketch of the physical problem.

The continuity, momentum, and energy equations are given by

$$\frac{\partial u}{\partial x} + \frac{\partial \upsilon}{\partial y} = 0, \tag{2}$$

$$u\frac{\partial u}{\partial x} + \upsilon\frac{\partial u}{\partial y} = \nu\left(1 + \frac{1}{\beta}\right)\frac{\partial^2 u}{\partial y^2}, \tag{3}$$

$$u\frac{\partial T}{\partial x} + \upsilon\frac{\partial T}{\partial y} = \kappa\frac{\partial^2 T}{\partial y^2}. \tag{4}$$

In the above equations, u and v are the components of velocity in the x and y directions, respectively, ν is the kinematic viscosity, $\beta = \mu_{\mathrm{B}}\sqrt{2\pi_{\mathrm{c}}}/p_y$ is the parameter of the Casson fluid, T

is the temperature of the fluid, and κ is the thermal diffusivity of the fluid.

2.1. Boundary conditions

At the very beginning, i.e., at the initial state when the transpiration starts, the surface temperature is assumed constant. The appropriate boundary conditions are

$$u = U = cx,\ v = -V_0,\ T = T_w, \quad \text{at} \quad y = 0, \tag{5}$$

$$u \to 0, \quad T \to T_\infty, \quad \text{as} \quad y \to \infty. \tag{6}$$

Here $c > 0$ is the rate of stretching, T_w is the uniform temperature of the sheet, T_∞ is the free stream temperature, and V_0 is a constant representing the velocity of suction ($V_0 > 0$) or the velocity of blowing ($V_0 < 0$).

2.2. Solution

By using

$$\eta = y\sqrt{\frac{c}{\nu}}, \quad u = cxf'(\eta),$$

$$v = -\sqrt{c\nu}f(\eta), \quad \frac{T - T_\infty}{T_w - T_\infty} = \theta(\eta), \tag{7}$$

Equation (2) is automatically satisfied, while Eqs. (3)–(6) yield

$$\left(1 + \frac{1}{\beta}\right) f''' + ff'' - f'^2 = 0, \tag{8}$$

$$\theta'' + Prf\theta' = 0, \tag{9}$$

$$f' = 1, \quad f = S, \quad \theta = 1, \quad \text{at} \quad \eta = 0, \tag{10}$$

$$f' \to 0, \quad \theta \to 0, \quad \text{as} \quad \eta \to \infty, \tag{11}$$

where the prime denotes the differentiation with respect to η; η is the similarity variable; θ is the non-dimensional temperature; $S = V_0/\sqrt{c\nu}$ is the transpiration parameter, which corresponds to suction or blowing according to $S > 0$ or < 0; and $Pr = \nu/\kappa$ is the Prandtl number.

Let

$$f(\eta) = a + b\mathrm{e}^{-\alpha\eta} \tag{12}$$

be the solution of Eq. (8) subject to the conditions

$$f(0) = S, \quad f'(0) = 1, \quad f'(\infty) = 0. \tag{13}$$

Substituting Eq. (12) into Eqs. (8) and (13) yields

$$a = S + \frac{1}{\alpha}, \quad b = -\frac{1}{\alpha},$$

where α satisfies the equation

$$\left(1 + \frac{1}{\beta}\right)\alpha^2 - S\alpha - 1 = 0. \tag{14}$$

Thus the exact solution of Eq. (8) subject to the corresponding boundary conditions is given by

$$f(\eta) = S + \frac{2(1+1/\beta)}{S \pm \sqrt{S^2 + 4(1+1/\beta)}} - \frac{2(1+1/\beta)}{S \pm \sqrt{S^2 + 4(1+1/\beta)}} \times \exp\left(-\frac{S \pm \sqrt{S^2 \pm 4(1+1/\beta)}}{2(1+1/\beta)}\eta\right). \tag{15}$$

Substituting the solution for the momentum equation in Eq. (9), we obtain

$$\theta'' + Pr\left\{S + \frac{2(1+1/\beta)}{S \pm \sqrt{S^2 + 4(1+1/\beta)}} - \frac{2(1+1/\beta)}{S \pm \sqrt{S^2 + 4(1+1/\beta)}} \times \exp\left(-\frac{S \pm \sqrt{S^2 \pm 4(1+1/\beta)}}{2(1+1/\beta)}\eta\right)\right\}\theta' = 0. \tag{16}$$

To obtain the solution of the thermal field, we adopt the new variable $\xi = -\frac{Pr}{\alpha^2}\mathrm{e}^{-\alpha\eta}$. Substituting this variable in Eq. (9), we obtain

$$\xi\frac{\partial^2\theta}{\partial\xi^2} + (1 - Pr - \xi)\frac{\partial\theta}{\partial\xi} = 0.$$

The corresponding boundary conditions become

$$\theta\left(\xi = -\frac{Pr}{\alpha^2}\right) = 1, \quad \theta(\xi = 0) = 0.$$

The temperature distribution can be obtained by using Kummer's function M_1 in terms of η

$$\theta(\eta) = \mathrm{e}^{-\delta\eta}\frac{M_1\left(\frac{\chi_0 + Z_0 - 4}{2},\ 1 + Z_0,\ -\frac{Pr}{\alpha^2}\mathrm{e}^{-\alpha\eta}\right)}{M_1\left(\frac{\chi_0 + Z_0 - 4}{2},\ 1 + Z_0,\ -\frac{Pr}{\alpha^2}\right)},$$

where $\delta = (\chi_0 + Z_0)/2$, $\chi_0 = Pr/\alpha^2$, $Z_0 = \chi_0$. Thus,

$$\theta(\eta) = \mathrm{e}^{-\frac{Pr}{\alpha^2}\eta}\frac{M_1\left(\frac{Pr}{\alpha^2} - 2,\ 1 + \frac{Pr}{\alpha^2},\ -\frac{Pr}{\alpha^2}\mathrm{e}^{-\eta}\right)}{M_1\left(\frac{Pr}{\alpha^2} - 2,\ 1 + \frac{Pr}{\alpha^2},\ -\frac{Pr}{\alpha^2}\right)} \tag{17}$$

is the solution of Eq. (4), where α is given by Eq. (14).

3. Results and discussion

In order to analyze the results, numerical computations have been carried out for various values of the Casson parameter β, the transpiration parameter S, and the Prandtl number Pr. For illustrations of the results, the numerical data are plotted in Figs. 2–6.

Let us first concentrate on the effects of the Casson parameter β on the velocity and temperature profiles in the absence of transpiration at the wall. Figures 2(a) and 2(b) depict the effects of the Casson parameter β on the velocity and temperature profiles for a non permeable sheet (i.e., in the absence of suction/blowing). The velocity is found to decrease as the Casson parameter β increases, whereas the temperature increases in this case. Decreasing thickness of the momentum boundary layer with increasing β is noted, while the thermal boundary layer thickens with increasing β.

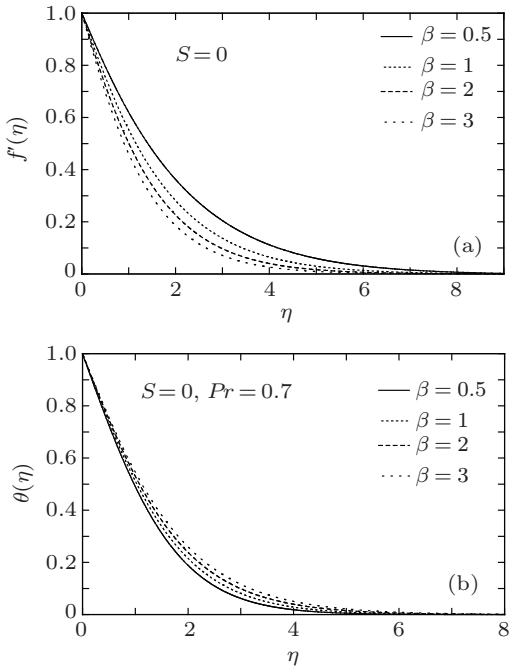


Fig. 2. Variations of (a) velocity $f'(\eta)$ and (b) temperature $\theta(\eta)$ with η for several values of Casson parameter β in the absence of transpiration.

Figures 3(a) and 3(b) display the velocity and temperature profiles for variable values of the Casson parameter β in the presence of transpiration at the wall, i.e., for a permeable stretching sheet. The fluid velocity is found to decrease as the Casson parameter β increases for both cases (Fig. 3(a)), whereas the temperature at a point increases with increasing β (Fig. 3(b)). The fluid velocity is much more suppressed in the case of suction ($S = 0.5$) than that in the case of blowing ($S = -0.5$) (Fig. 3(a)). On the other hand, the increase in the temperature field is much more pronounced in the case of blowing ($S = -0.5$) than that with suction ($S = 0.5$) (Fig. 3(b)).

Figures 4(a) and 4(b) show the effects of the transpiration parameter S on the velocity and temperature profiles, respectively. It is observed that the velocity decreases significantly with increasing suction, whereas the fluid velocity is found to increase as blowing increases (Fig. 4(a)). It is observed that when the wall suction ($S > 0$) is considered, a decrease is seen in the boundary layer thickness and the velocity field is reduced. The increased suction causes progressive thinning of the boundary layer. However, injection ($S < 0$) has the opposite effect. The physical explanation for such a behavior is as follows. When stronger blowing is provided, the heated fluid is pushed further away from the wall where, due to a reduced influence of viscosity, the flow accelerates. This increases the maximum velocity within the boundary layer. The same principle operates, but in the reverse way, in the case of suction. Here $S = 0$ represents the case of a non porous stretching sheet. Figure 4(b) represents the temperature profiles for variable values of the transpiration parameter S. It is seen that the temperature decreases with increasing suction, whereas it increases with blowing (Fig. 4(b)). Actually, the effect of suction is to make the velocity and temperature distributions more uniform within the boundary layer. The imposition of fluid suction at the surface has a tendency to reduce both the momentum and thermal thicknesses of the boundary layer where the viscous effects dominate. This reduces both the fluid velocity and temperature. On the other hand, the thermal boundary layer thickness increases with injection, which causes a decrease in the rate of heat transfer.

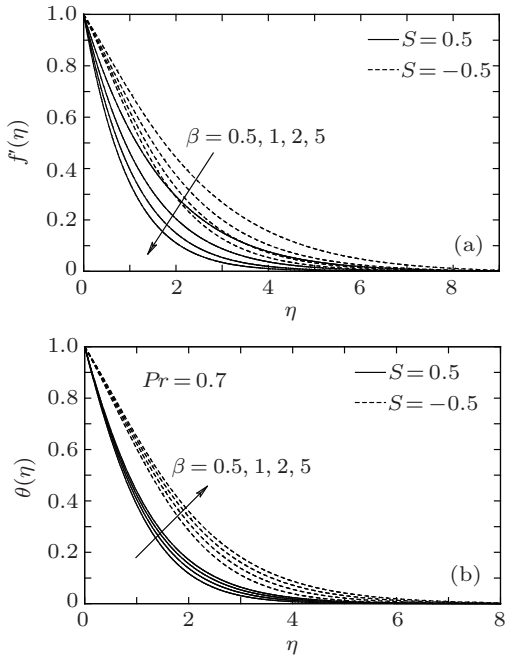


Fig. 3. Variations of (a) velocity $f'(\eta)$ and (b) temperature $\theta(\eta)$ with η for several values of Casson parameter β in the presence of transpiration.

Figure 5(a) depicts the effects of the Prandtl number Pr on the temperature profile in the absence of transpiration ($S = 0$) at the boundary. The temperature decreases with increasing Pr. An increase in the Prandtl number reduces the thermal boundary layer thickness. The Prandtl number is the ratio of momentum diffusivity to thermal diffusivity. In heat transfer problems, Pr controls the relative thickening of the momentum and thermal boundary layers. When Pr is small, heat diffuses quickly compared to the velocity (momentum), which means that for liquid metals, the thickness of the thermal boundary layer is much larger than that of the momentum boundary layer. Fluids with lower Prandtl numbers have higher thermal conductivities (and thicker thermal boundary layer structures) so that heat can diffuse from the sheet faster than that for higher-Pr fluids (thinner boundary layers). Hence the Prandtl number can be used to determine the rate of cooling in conducting flows. It is well known that if the Prandtl number is greater than 1, the thermal boundary layer is thinner than the velocity boundary layer. If the Prandtl number is less than 1, which is the case for air under standard conditions, the thermal

boundary layer is thicker than the velocity boundary layer. For the Casson fluid, the momentum diffusion is low, so in this case, the thermal boundary layer formation may also have a small Prandtl number. Figure 5(b) shows the nature of temperature profiles for variable values of the Prandtl number in the presence of transpiration ($S = 0.5, -0.5$). Here the temperature also decreases with increasing Pr (Fig. 5(b)). Moreover, the thermal boundary layer thickness decreases as the Prandtl number increases (Fig. 5(b)).

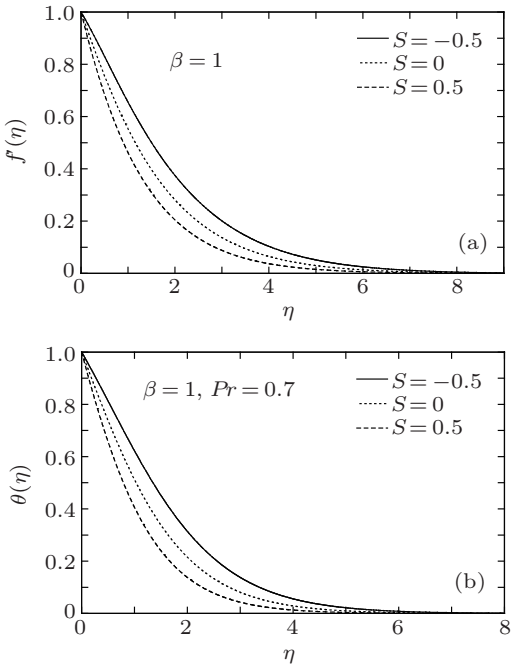


Fig. 4. Variations of (a) velocity $f'(\eta)$ and (b) temperature $\theta(\eta)$ with η for several values of transpiration parameter S.

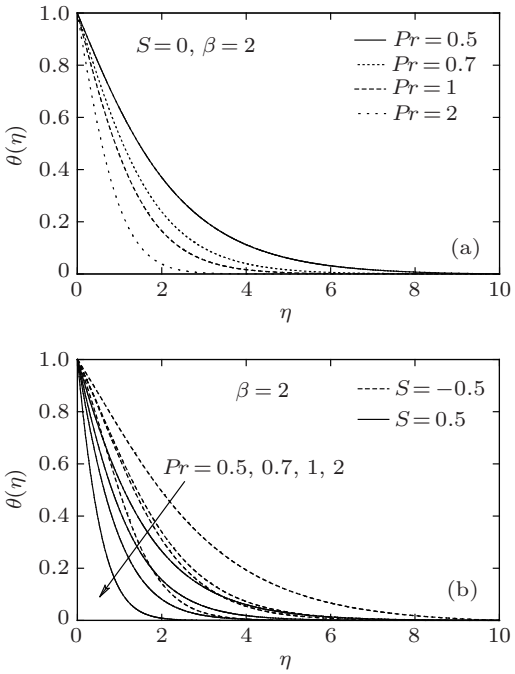


Fig. 5. Variations of temperature $\theta(\eta)$ with η for several values of Prandtl number Pr in the (a) absence or (b) presence of transpiration.

Figure 6(a) exhibits the nature of the skin-friction coefficient with the Casson parameter β for three values of the suction/blowing parameter S. It is found that the skin-friction coefficient increases with increasing β, and its magnitude is higher for suction than for blowing. From this figure, it is very clear that $f''(0)$ is negative here, which is consistent with the present case, as a stretching sheet that induces the flow is considered here. Physically, a negative sign of $f''(0)$ implies that the surface exerts a dragging force on the fluid, and a positive sign implies the opposite (i.e., lift force). Figure 6(b) displays the nature of the heat transfer coefficient $\theta'(0)$ against the Casson parameter β. An increase in β leads to an increase in the heat transfer coefficient. The wall temperature gradient $\theta'(0)$ increases with blowing but decreases with suction (Fig. 6(b)).

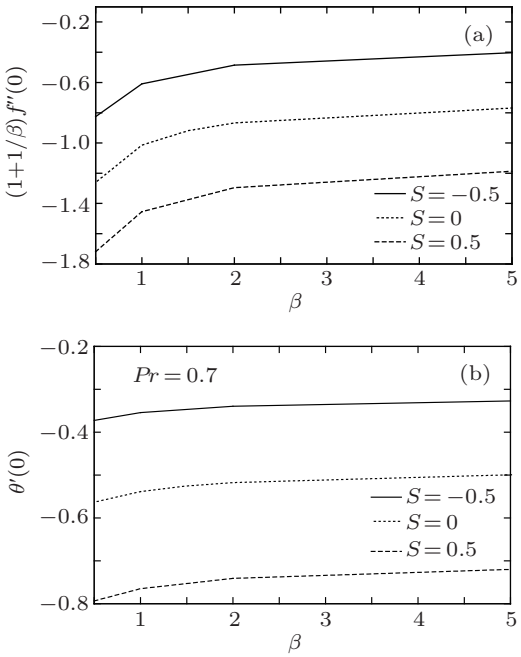


Fig. 6. (a) Skin-friction coefficient and (b) wall temperature gradient $\theta'(0)$ versus Casson parameter β for different transpiration parameter S.

4. Conclusions

The present study provides the exact solutions for the steady boundary layer flow and heat transfer of a Casson fluid over a linearly stretching surface. The main findings of this investigation can be summarized as follows.

(i) The effect of the suction parameter is to suppress the velocity field, which in turn enhances the skin-friction coefficient.

(ii) The thermal boundary layer in case of suction ($S > 0$) is thinner than that in case of impermeability ($S = 0$). However, it is thicker in the case of blowing ($S < 0$).

(iii) The momentum boundary layer thickness decreases as the Casson parameter increases, however the thermal boundary layer thickens in this case.

(iv) The surface shear stress increases as the Casson parameter increases.

(v) With increasing Pr, the temperature decreases and the thickness of the thermal boundary layer is reduced.

References

[1] Pal D 2009 *Meccanica* **44** 145
[2] Mahapatra T R, Dholey S and Gupta A S 2007 *Int. J. Non-Linear Mechanics* **42** 484
[3] Sajid M, Hayat T and Asghar S 2007 *Int. J. Heat Mass Transfer* **50** 1723
[4] Crane L J 1970 *Zeit. Angew. Math. Mech.* **21** 645
[5] Carragher P and Crane L J 1982 *Zeit. Angew. Math. Mech.* **62** 564
[6] Gupta P S and Gupta A S 1977 *Can. J. Chem. Engng.* **55** 744
[7] Abel M S, Datti P S and Mahesha N 2009 *Int. J. Heat Mass Transfer* **52** 2902
[8] Mukhopadhyay S 2010 *Chin. Phys. Lett.* **27** 124401
[9] Bhattacharyya K, Mukhopadhyay S and Layek G C 2011 *Chin. Phys. Lett.* **28** 094702
[10] Bhattacharyya K, Hayat T and Alsaedi A 2013 *Chin. Phys. B* **22** 024702
[11] Abel M S and Mahesha N 2008 *Applied Mathematical Modelling* **32** 1965
[12] Ellahi R, Hayat T, Mahomed F M and Zeeshan A 2010 *Z. Angew. Math. Phys.* **61** 877
[13] Hsiao K L 2007 *Appl. Thermal Engng.* **27** 1895
[14] Andersson H I and Dandapat B S 1992 *Appl. Anal. Continuous Media* **1** 339
[15] Hassanien I A 1996 *Appl. Model.* **20** 779
[16] Sadeghy K and Sharifi M 2004 *Int. J. Non-linear Mech.* **39** 1265
[17] Serdar B and Salih Dokuz M 2006 *Int. J. Engng Sci.* **44** 49
[18] Haroun M H 2007 *Commun. Nonlinear Sci. Numer. Simulat.* **12** 1464
[19] Hayat T, Iqbal Z and Mustafa M 2012 *J. Mech.* **28** 209
[20] Sajid M, Ahmad I, Hayat T and Ayub M 2009 *Commun. Nonlinear Sci. Numer. Simulat.* **14** 96
[21] Heyhat M M and Khabazi N 2010 *Proc. IMechE* Vol. **225** Part C: J. Mechanical Engineering Science
[22] Hayat T, Awais M and Sajid M 2011 *Int. J. Mod. Phys. B* **25** 2863
[23] Mukhopadhyay S 2012 *Chin. Phys. Lett.* **29** 054703
[24] Fung Y C 1984 *Biodynamics Circulation* (New York: Springer-Verlag)
[25] Dash R K, Mehta K N and Jayaraman G 1996 *Int. J. Engng Sci.* **34** 1145
[26] Eldabe N T M and Salwa M G E 1995 *J. Phys. Soc. Jpn.* **64** 41
[27] Boyd J, Buick J M and Green S 2007 *Phys. Fluids* **19** 93
[28] Mukhopadhyay S 2009 *Int. J. Heat Mass Transfer* **52** 3261
[29] Mukhopadhyay S 2011 *Nuc. Eng. Des.* **241** 2660
[30] Mukhopadhyay S and Vajravelu K 2012 *ASME J. Appl. Mech.* **79** 044508
[31] Mukhopadhyay S and Layek G C 2008 *Int. J. Heat Mass Trans.* **51** 2167
[32] Mukhopadhyay S and Gorla R S R 2012 *Heat Mass Transfer* **48** 1773
[33] Ishak A, Nazar R and Pop I 2009 *Chem. Engng. J.* **148** 63
[34] Bhattacharyya K, Mukhopadhyay S, Layek G C and I Pop 2012 *Int. J. Heat Mass Transfer* **55** 2945